AGU PUBLICATIONS

Geophysical Research Letters

RESEARCH LETTER
10.1002/2014GL061872

Key Points:
- Non-similar earthquakes in and around the repeater should be counted for slip
- Aging-law can explain the aperiodicity off Kamaishi even for a single asperity
- The large post-seismic slip off Kamaishi may propagate from ESE to WNW

Supporting Information:
- Readme
- Text S1
- Text S2
- Figure S1
- Figure S2

Correspondence to:
K. Ariyoshi,
ariyoshi@jamstec.go.jp

Citation:
Ariyoshi, K., N. Uchida, T. Matsuzawa, R. Hino, A. Hasegawa, T. Hori, and Y. Kaneda (2014), A trial estimation of frictional properties, focusing on aperiodicity off Kamaishi just after the 2011 Tohoku earthquake, *Geophys. Res. Lett.*, *41*, 8325–8334, doi:10.1002/2014GL061872.

Received 24 SEP 2014
Accepted 14 NOV 2014
Accepted article online 18 NOV 2014
Published online 15 DEC 2014

A trial estimation of frictional properties, focusing on aperiodicity off Kamaishi just after the 2011 Tohoku earthquake

Keisuke Ariyoshi[1], Naoki Uchida[2], Toru Matsuzawa[2], Ryota Hino[3], Akira Hasegawa[2], Takane Hori[1], and Yoshiyuki Kaneda[4]

[1]Research and Development Center for Earthquake and Tsunami, Japan Agency for Marine-Earth Science and Technology, Yokohama, Japan, [2]Research Center for Prediction of Earthquakes and Volcanic Eruptions, Graduate School of Science, Tohoku University, Sendai, Japan, [3]International Research Institute of Disaster Science, Tohoku University, Sendai, Japan, [4]Disaster Mitigation Research Center, Nagoya University, Nagoya, Japan

Abstract Motivated by the fact that temporal earthquake aperiodicity was observed off Kamaishi just after the 2011 Tohoku earthquake, we performed numerical simulations of chain reactions due to the postseismic slip of large earthquakes by applying rate- and state-dependent friction laws. If the repeater is composed of single asperity, our results show that, (i) a mixture of partial and whole rupturing of a single asperity can explain some of the observed variability in timing and size of the repeating earthquakes off Kamaishi; (ii) the partial rupturing can be reproduced with moderate frictional instability with the aging-law and not the slip or Nagata laws; (iii) the perturbation of the activated earthquake hypocenters observed mostly in the ESE-WNW direction may reflect the fact that the large postseismic slip of the 2011 Tohoku earthquake propagated from ESE to WNW off Kamaishi; (iv) the observed region of repeating earthquake quiescence may reflect the strong plate coupling of megathrust earthquakes.

1. Introduction

Analysis of repeating earthquakes (repeaters) has been a useful tool to monitor the slip velocity field on worldwide plate boundaries driven by preseismic [e.g., *Kato et al.*, 2012] and postseismic slip [e.g., *Uchida et al.*, 2009]. A major example is the well-known repeater sequence off Kamaishi (Figure 1a) with a characteristic interval of about 5 years [*Matsuzawa et al.*, 2002], seismic magnitude of about *M*4.8 (Figure 1b) and spatial slip distribution [*Shimamura et al.*, 2011a] that has been explained by an isolated asperity model [*Igarashi et al.*, 2001].

Just after the 2011 Tohoku earthquake, however, *Ye et al.* [2012] reported that temporal earthquake aperiodicity occurred off Kamaishi, with recurrence intervals much shorter than anticipated (about 9 days at shortest) and magnitude greater (e.g., *M*5.9) and smaller (e.g., *M*4.3) than the characteristic earthquake, as shown in Figure 1b. The greater earthquakes are thought to be attributed to the fast loading of repeaters due to the rapid postseismic slip [e.g., *Chen et al.*, 2010]. For the smaller earthquakes, however, this model does not hold simply. *Ye et al.* [2012] thought that the greater and the smaller earthquakes originate from different asperities. If so, then it is not clear why the smaller asperities ruptured just once (*M*4.3 on 29 March) and not continuously.

Recently, *M*5-class repeaters in subduction zones have been found off Kushiro [*Sakoi et al.*, 2012] and near Miyako Island [*Tamaribuchi et al.*, 2010], where both the repeater cycles are also complex. This is probably due to large earthquakes nearby such as the inshore Yonaguni Island earthquake (near Miyako Island) in 1966 (*M*7.8) [*The Headquarters for Earthquake Research Promotion*, 2004] and Tokachi earthquakes in 1952 (*M*8.2) and 2003 (*M*8.0) [*Yamanaka and Kikuchi*, 2003]. Therefore, to model the complex earthquake cycle in these regions, it is important to understand the temporal aperiodicity off Kamaishi.

In this study, we formulate a simplified model for the long-term cycle for repeaters perturbed by the passage of large postseismic slip generated from a nearby large earthquake in a subduction zone to explain the temporal aperiodicity and extract the frictional properties and characteristics of the complex earthquake cycle.

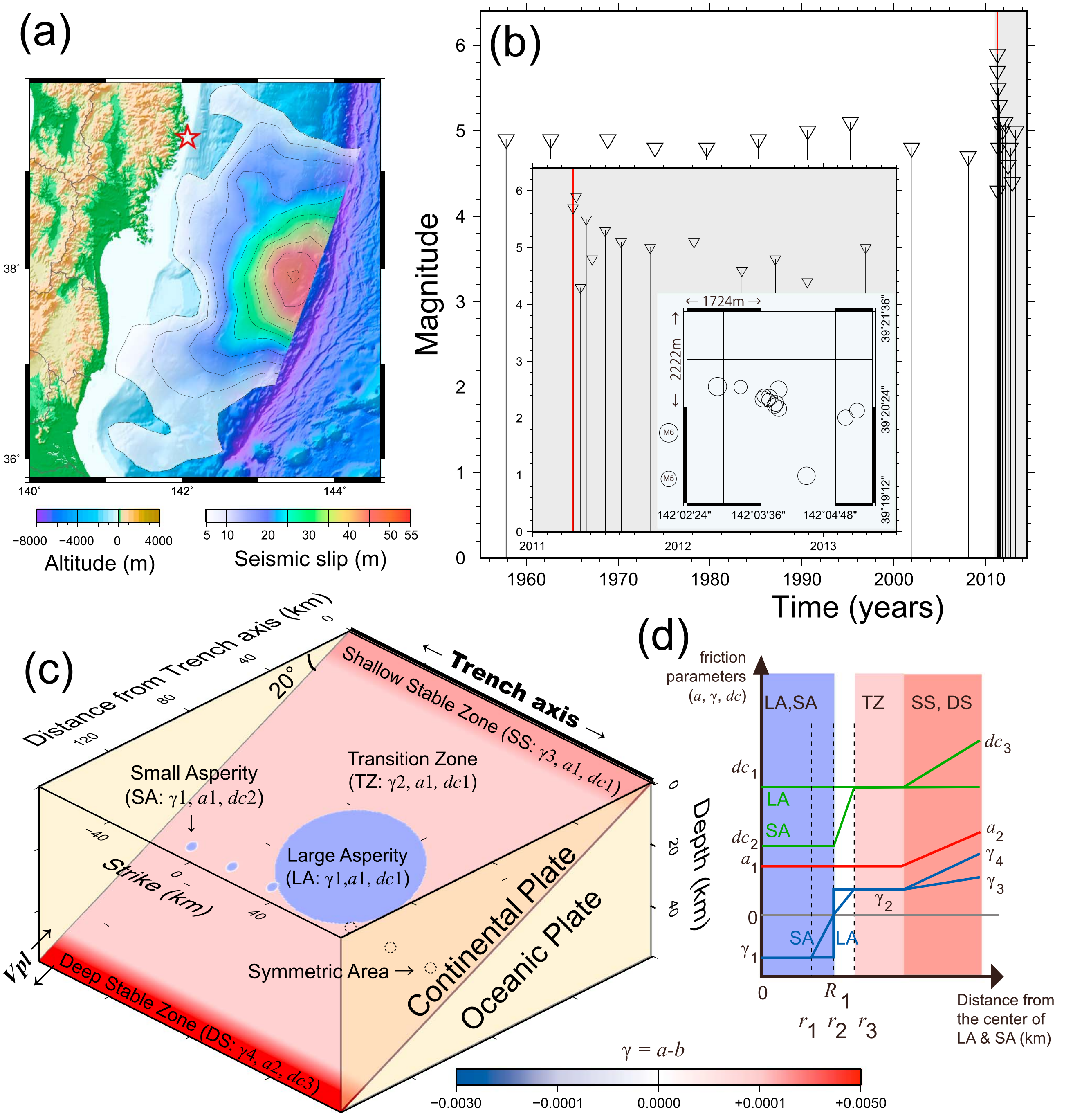

Figure 1. (a) Bathymetric map showing the epicenters of repeaters off Kamaishi marked by the red star. The total slip distribution of larger than 5 m of the 2011 Tohoku earthquake from *Yagi and Fukahata* [2011] is superposed. (b) Magnitude-time plot for the off Kamaishi region with close-up in the gray-colored time window and its epicenter map estimated by *Shimamura et al.* [2011b]. The vertical red line shows the occurrence time of the 2011 Tohoku earthquake. (c) Schematic view of the 3-D simulation model of a subduction plate boundary with frictional parameter $\gamma = a - b$. Radii for LA and SA are ($R_1 = 30$) and (r_1, r_2, $r_3 = 1.5, 2, 2.5$) (km), respectively. Aspect ratios of LA and SA are 0.8 and 1.0, respectively. Dashed circles represent the symmetric area for SA along strike. (d) Frictional parameters with respect to distance from the center of LA and SA. The values of the frictional parameters ($\gamma_1, \gamma_2, \gamma_3, \gamma_4; a_1, a_2$) = ($-7.8, +1.0, +8.0, +49; 20, 50$) [$\times 10^{-4}$] and characteristic slip distance ($d_{c1}{}^{slip}$, $d_{c1}{}^{others}$, $d_{c2}{}^{aging}$, $d_{c2}{}^{Nagata}$, $d_{c2}{}^{slip}$, d_{c3}) = (0.09, 0.03, 0.006, 0.005, 0.012, 3.0) (m) are based on rock laboratory results [e.g., *Blanpied et al.*, 1998].

2. Numerical Model

In the proposed model, a reverse-type fault on a subduction plate interface is embedded in a homogeneous elastic half-space, dipping at 20° and extending 165 km from the free surface in the downdip direction (Figure 1c). The details of the numerical simulation method are described in Text S1 in the supporting information.

To perform trial simulations of the perturbed cycle of repeaters, we assume that the frictional coefficient μ obeys one of rate- and state-dependent friction (RSF) laws [*Dieterich*, 1979; *Ruina*, 1983],

$$\mu\sigma = \mu(\rho_r - \rho_w)gz = [\mu_0 + \{a\ln(V/V_0) + \Theta\}](\rho_r - \rho_w)gz, \tag{1}$$

$$\frac{\mathrm{d}\Theta}{\mathrm{d}t} = \frac{bV_0}{d_c}\left\{\exp\left(-\frac{\Theta - \mu_0}{b}\right) - \frac{V}{V_0}\right\} - c\frac{\mathrm{d}\mu}{\mathrm{d}t}, \tag{2}$$

$$\frac{\mathrm{d}\Theta}{\mathrm{d}t} = -\frac{V}{d_c}\left\{\Theta - \mu_0 + b\ln\left(\frac{V}{V_0}\right)\right\}, \tag{3}$$

where the effective normal stress σ is the difference between lithostatic and pore pressures, ρ_r and ρ_w are the densities of rock and water, respectively, g is the gravitational acceleration, z is the depth from the free surface, a and b are frictional parameters of stability, d_c is the critical slip distance, μ_0 is the nominal friction at steady state when the slip velocity $V = V_0$, Θ is a state variable. For the coefficient of stress weakening $c = 0$ and 2 in equation (2), we use the aging and Nagata laws [*Nagata et al.*, 2012], respectively, and for equation (3) we use the slip law [*Ampuero and Rubin*, 2008].

In this study, an asperity denotes a region with $a - b = \gamma < 0$, following *Boatwright and Cocco* [1996]. The plate interface is demarcated into five regions, as shown in Figure 1c: (i) large asperity (LA), (ii) small asperity (SA), (iii) transition zone (TZ), (iv) shallow stable zone (SS), and (v) deep stable zone (DS). The three different SAs along the strike direction (from LA) are defined as near (NSA), middle (MSA), and far distance asperity (FSA), with the same value of frictional instability $\sigma(b - a)/d_c$ [*Ruina*, 1983] because of the same depth. The values of the frictional parameters are the same between the three friction laws except the characteristic slip in LA (d_{c1}) and SA (d_{c2}) (Figure 1d) to make the magnitude of the earthquakes occurring in LA and SA as similar as possible, which is discussed later.

3. Results

For a single asperity model in which LA or SA exist alone, the recurrence intervals (T_r or t_r in year), the moment magnitudes (M_w or m_w, where the seismic slip denotes slip faster than 1 mm/s) and the stress drop averaged in LA or SA ($\Delta\Sigma$ or $\Delta\sigma$ in MPa, where effective normal stress at the center of LA and SA are 469 and 586 MPa, respectively) are (T_r, M_w; t_r, m_w; $\Delta\Sigma$, $\Delta\sigma$) = $(62.9, 7.7; 2.5, 3.8; 7.0, 2.1)^{\mathrm{aging}}$, $(69.8, 7.8; 7.0, 5.3; 6.3, 6.2)^{\mathrm{Nagata}}$, $(82.5, 7.9; 6.3, 5.3; 7.0, 6.3)^{\mathrm{slip}}$ for each of the three RSF law models.

In the case of MSA and FSA as shown in Figure 1c, the values of T_r and M_w are almost the same as in the single asperity model because of the negligible stress perturbation of SA on LA, while they are also nearly constant but slightly different in the case of NSA: (T_r, M_w) = $(64.5 \pm 0.4, 7.7)^{\mathrm{aging}}$, $(68.2 \pm 0.4, 7.8)^{\mathrm{Nagata}}$, $(82.3, 7.9)^{\mathrm{slip}}$, because of the nonnegligible stress perturbation.

Figure 2 shows the time histories of the friction coefficient and common logarithm of the normalized slip velocity averaged over SA. Figures 2c and 2h show the temporal earthquake aperiodicity in MSA during postseismic slip passage as reproduced by the aging-law. Compared with Figure 2c, Figure 2a shows that similar slip events do not occur in NSA, which is discussed later. Figures 2b and 2g show the recurrence interval of temporal earthquake aperiodicity in FSA to be about several tens of days, which is much longer than that for MSA (Figure 2h).

Figure 3 shows snapshots of the normalized slip velocity field for the aging law, which indicates that the gap in the color of the slip velocity field is clear in and around MSA and FSA for all events. However, this does not hold for NSA except for Event F, because of the strong stress shadow [e.g., *Johnson*, 2013] from LA as indicated by the double-headed blue arrow in Figure 2a. To see the effect of the stress shadow, we treat the normalized slip velocity averaged in the symmetric area for SA along the strike direction (see Figure 1c) as the background slip velocity, which is shown by the dashed orange lines in Figure 2. Figure 2f shows that the

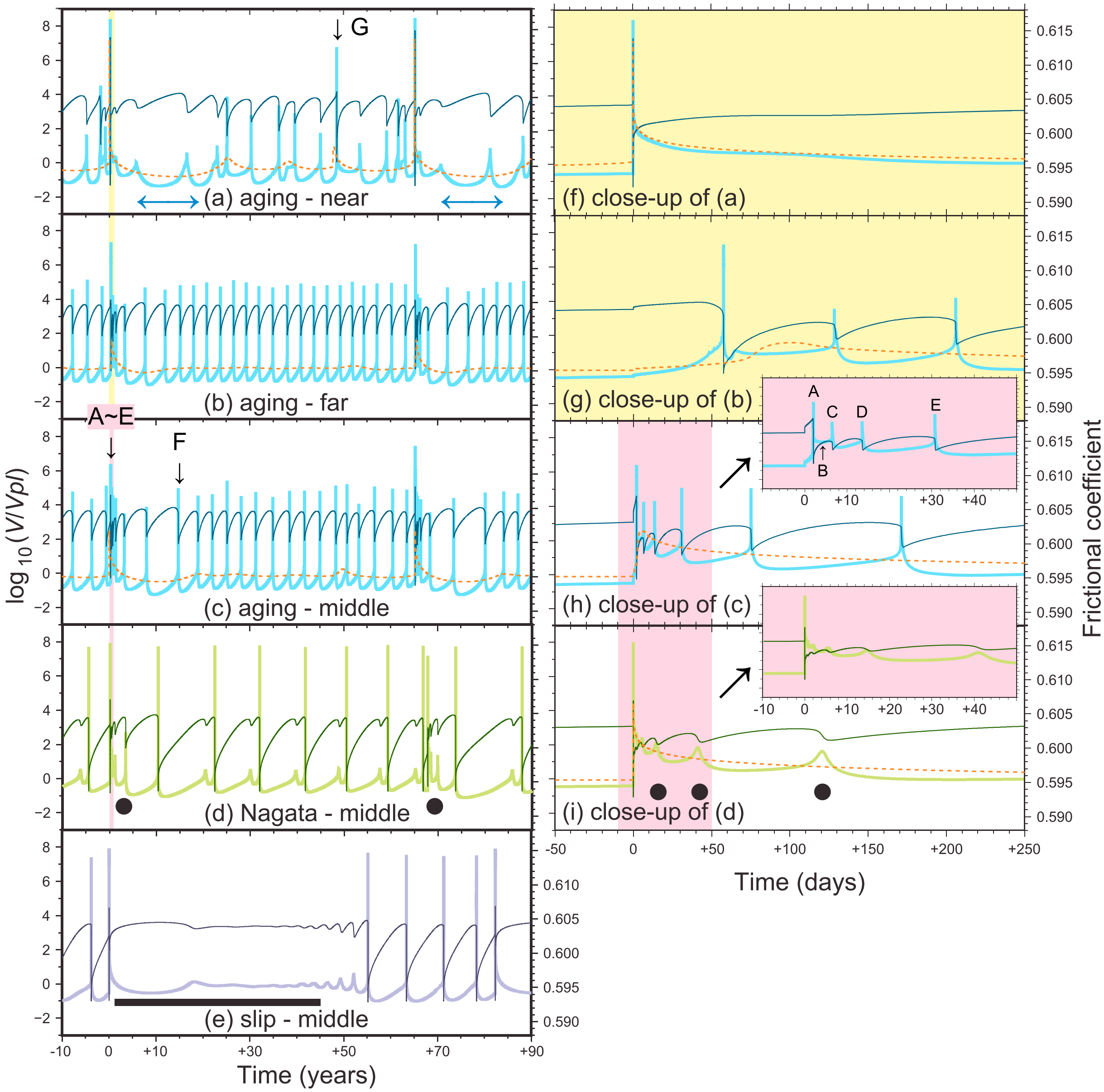

Figure 2. Time histories of the friction coefficient, or shear stress normalized by the effective normal stress, (thin line) and the slip velocity normalized with respect to V_{pl} on a common-logarithmic-scale (bold line) averaged over SA. The origin time ($t = 0$) is set to the occurrence of the large earthquake in LA. Adopted friction laws are the (a–c, f–h) aging (cyan), (d, i) Nagata (lime green), and (e) slip (purple). The location of SA is (Figures 2a and 2f) near, (Figure 2b and 2g) far, and (Figures 2c–2e, 2h, and 2i) middle distance from LA in Figure 1. Orange dashed lines denote the normalized slip velocity averaged in the symmetric area for SA along the strike direction as shown in Figure 1c. (Figures 2f–2i) Close-up of the time window with yellow in Figures 2a and 2b and magenta in Figures 2c and 2d, respectively. Double-headed blue arrow indicates seismic quiescence for NSA due to strong plate coupling in LA. Black bold circles in Figures 2d and 2i and horizontal line in Figure 2e represent aseismic slip events and seismic quiescence, respectively. Events labeled A–F in Figures 2c and 2h and G in Figure 2a are analyzed in Figure 3 and Figure S2, respectively.

averaged slip velocity in NSA is almost the same as the background slip velocity. This means that the slip velocity field for NSA just before and after the large earthquake is mainly dominated by the stress field around LA rather than the frictional instability in NSA, which prevents NSA from the temporal earthquake activation. Moreover, Figure 2a shows that slip events in NSA are not characteristic but show various slip behaviors throughout the earthquake cycle of LA, which seems to correlate with the fluctuation of the slip velocity field around NSA as seen for Events F (Figure 3f) and G (Figure S2). This suggests that only nonsimilar earthquakes occur within a short range from the strong asperity rather than repeaters, which is discussed later.

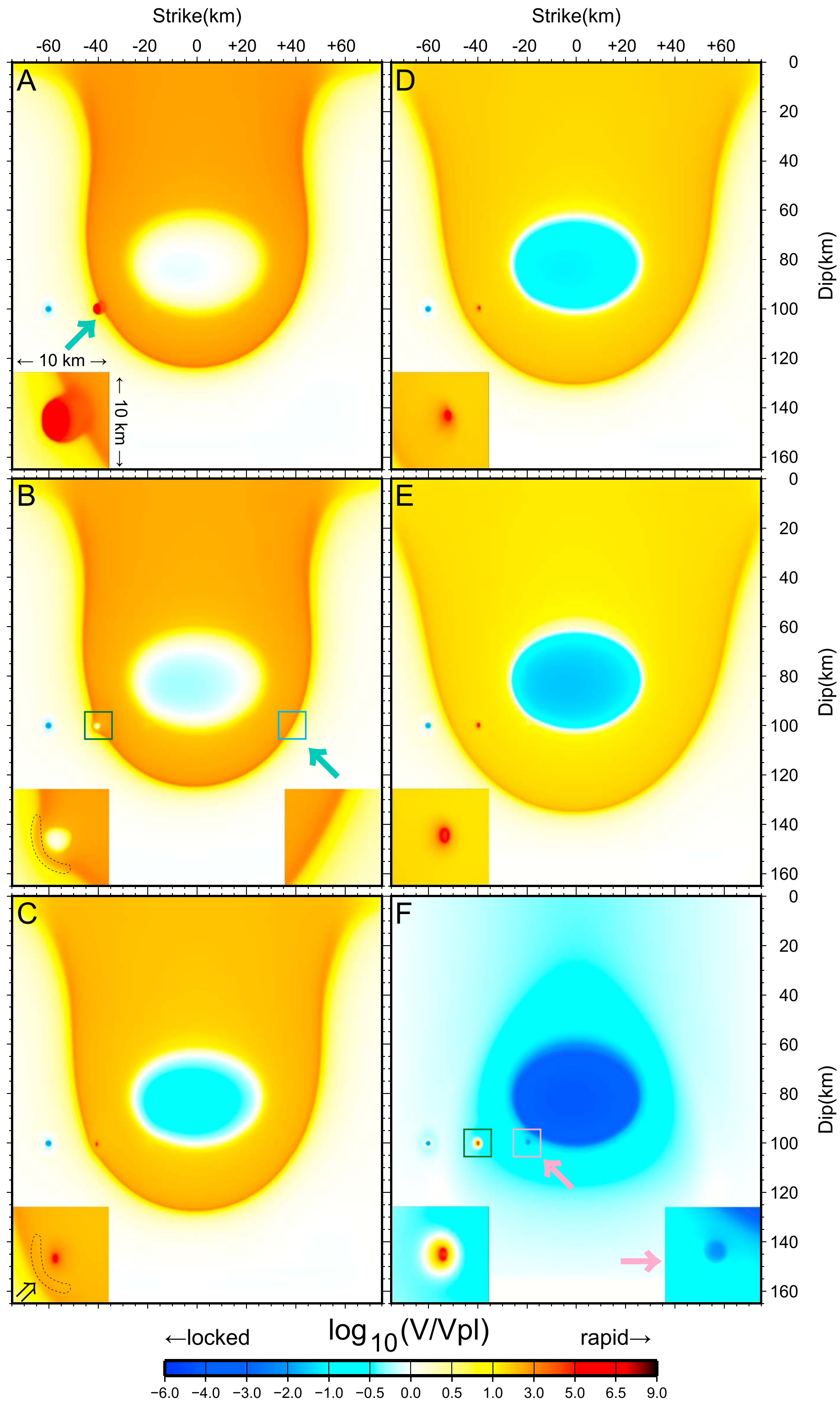

Figure 3. (a–f) Snapshots of the slip velocity normalized with respect to V_{pl} on a common-logarithmic scale for the coexistence model of the aging law at times labeled A to F in Figures 2c and 2h. The inset in the left side of each snapshot is a close-up of the slip velocity distribution in and around SA at the middle distance (MSA) in Figure 1. The inset in the right side of Shots B and F are along the strike symmetry of MSA and at the near distance (NSA) in Figure 1c, respectively. Closed broken curves in Figures 3b and 3c show the locally fast propagation of the postseismic slip driven by Event A. Black arrow in Figure 3c indicates the apparent stagnation of the propagation from Figure 3b.

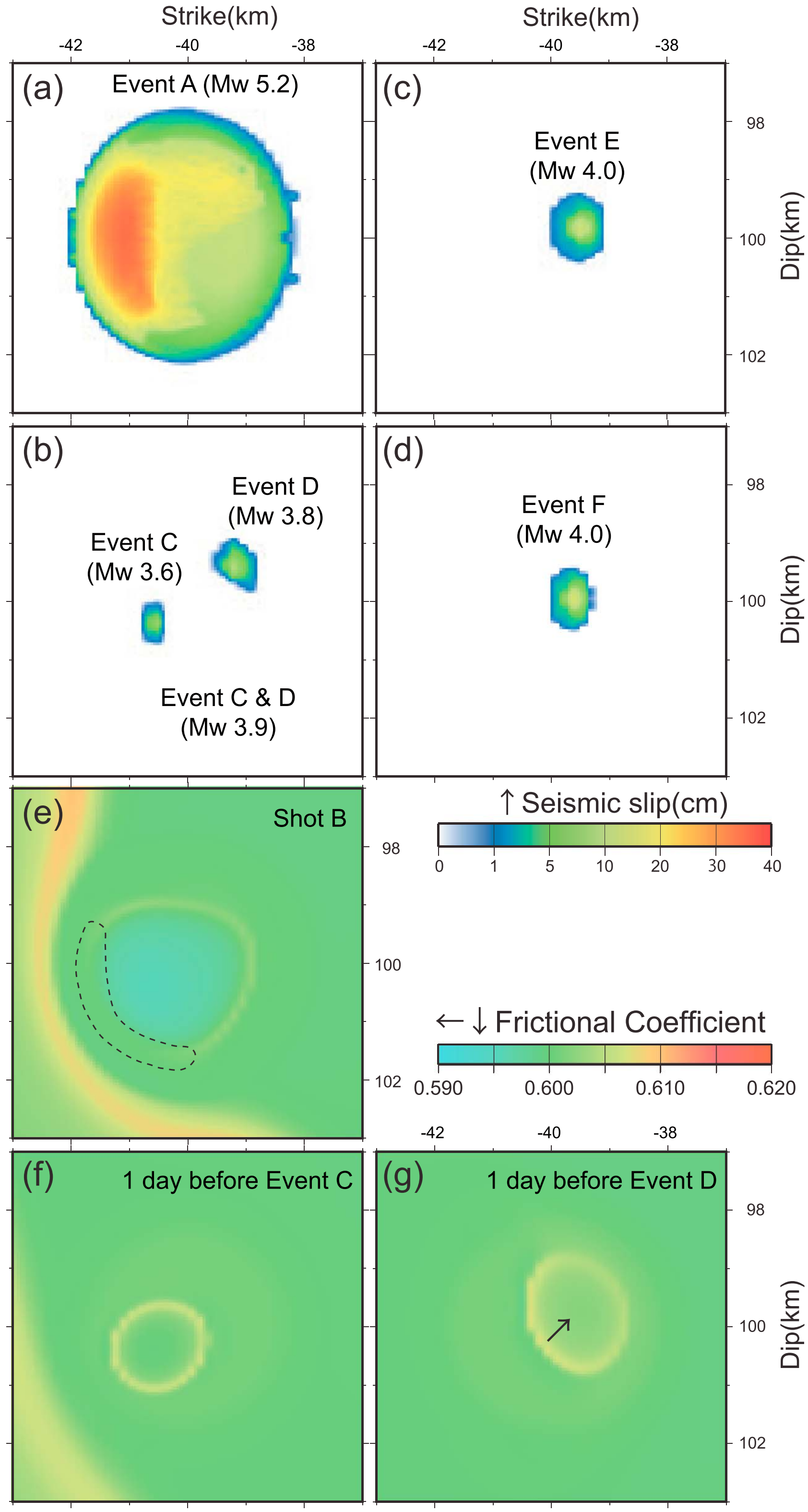

Figure 4. (a–d) Coseismic slip distribution for Events A and C–F in Figures 2c and 2h in MSA for the aging law. (e–g) Frictional coefficient distribution for Shot B and 1 day before Events C and D. Note that Events C and D are superimposed. Black closed curve in Figure 4e indicates low frictional coefficient. Black arrow in Figure 4g shows movement direction of high frictional coefficient.

Figures 4a to 4d show the coseismic slip distribution of Events A and C to F for MSA. Figures 4e to 4g show the frictional coefficient at Shot B, one day before Events C and D. In Figure 3a, the velocity field at the front of the postseismic slip is high, which promotes rupture for the whole MSA. Subsequently, the small postseismic slip of Event A is released locally around MSA, which causes the apparent propagation of large postseismic slip from LA and is locally faster around MSA as compared between the closed broken curve and the symmetric part in Figure 3b. This suggests a chain reaction process [*Matsuzawa et al.*, 2004]. Figure 4e shows the low frictional coefficient around MSA as indicated by the black closed curve, which is due to the stress release caused by the passage of large postseismic slip as shown by Figure 3b. After that, black arrow in Figure 3c shows that the propagation of the large postseismic slip temporarily stagnates around the outskirt of MSA, which heals shear stress in the low frictional coefficient zone and promote Event C partial rupture in the forward part of MSA as shown in Figures 4b and 4f. After 7 days, complementary slip in the backward part of MSA occurs as Event D because the postseismic slip of Event C propagates backward, as shown by the black arrow in Figure 4g. Because Event E is similar to the characteristic earthquake (e.g., Event F), the effect of the large postseismic slip passage on MSA is sufficiently attenuated at Event E. The moment magnitude for the sum of Events C and D (M_w 3.9) is smaller than that of the characteristic single earthquake (Events E and F) because aseismic (slower than 1 mm/s) slip is also released even at Shot B as shown in Figures 2h (slip higher than V_{pl}) and Figure 3b (warm color in the outer rim of MSA).

For the Nagata law, Figures 2d and 2i show that aseismic slip events occur in the passage of postseismic slip as indicated by the black bold circles. However, it is difficult for temporal activation of aperiodicity to occur in our model by changing the values of $(b - a)$ and ${d_{c2}}^{\mathrm{Nagata}}$ because of the narrower transition zone between creep and regular earthquakes than the aging law due to greater decrease of frictional strength [e.g., *Kame et al.*, 2013], as described in Text S2. A large postseismic slip activates aseismic (slow) slip events, which is consistent with the theoretical analysis stating that the step change of loading velocity triggers slow events in the case of the Nagata law [*Kame et al.*, 2012].

For the slip law, Figure 2e shows that seismic quiescence occurs just after the occurrence of megathrust earthquake as indicated by the horizontal black line, because slip events are always repeating earthquakes that rupture the whole of SA as in Event A in Figure 4. In the case of weaker frictional instability than our model by assuming a less negative value of γ_1, the slip event in SA becomes a steady creep at a rate nearly equal to the plate convergence rate, V_{pl}, as described in Text S2. For step-change increase ($V_1 \sim V_{\mathrm{pl}}$ to $V_2 \sim V_{\mathrm{seis}}$), the stress drop per slip distance for the slip law is significantly greater than that for the aging law [*Ampuero and Rubin*, 2008]. Hence, the slip law easily generates whole rupturing, rather than partial rupturing as in case of the aging law.

These results hold for different distances from LA (Text S2 and Figure S1) and different values of frictional parameters (γ_1 and d_{c3}) causing large earthquakes in the range of M_w about 7.5 to 8.0, which is described in Text S2.

4. Discussion

Because the observed temporal aperiodicity of repeating earthquakes can be reproduced with the aging law, we interpret the observations based on the simulation results. Without significant stress perturbation, the earthquake off Kamaishi is characteristic (about *M*4.8) and seismically ruptures in central part of SA like Event F.

After the 2011 Tohoku earthquake, GPS analysis suggested that the rapid postseismic slip had lasted for several to several tens of days [*Fukuda et al.*, 2013], which may have triggered the earthquake on 20 March (*M*5.9) that ruptured the whole of SA in its passage like Event A. Subsequently, the earthquake on 29 March (*M*4.3) may have ruptured the western part of SA like Event C. Because the *M*4.3 earthquake is in the west-northwestern part of the repeater [*Shimamura et al.*, 2011b], the large postseismic slip off Kamaishi may have propagated from east-southeast to west-northwest. This is consistent with the observations that the epicenters of the temporal earthquake aperiodicity fluctuate along the ESE - WNW direction (Figure 1b).

However, the slip event that ruptured the eastern part of SA like Event D has not been found yet. In addition, the frequency of the greater after-event was several times on 13 April (*M*5.5) and May 31 (*M*5.3) as shown in Figure 1b, which is inconsistent with our model for Event A occurring only once. These discrepancies might be

10.1002/2014GL061872

attributed to the modeling and the observational analysis. The amount and duration of the postseismic slip increase with increasing asperity size under the same friction conditions [e.g., *Kato*, 2007]; hence, the discrepancy of the greater earthquake frequency is likely due to the magnitude difference between the Tohoku earthquake (*M*9) and LA earthquake (*M*7.7) in our model. For simplicity, we neglected the effects of viscoelasticity [*Diao et al*., 2013], hierarchical asperity structure [*Hori and Miyazaki*, 2010], dynamic rupture [e.g., *Thomas et al*., 2014] and thermal pressurization [e.g., *Mitsui et al*., 2012], which should be considered in future studies.

From the seismic waveform inversion analysis, there is a small asperity in the western and central part of the *M*4.8 source region as a hierarchical structure [*Uchida et al*., 2007]. This means that the expected magnitude of the smaller earthquake in the eastern part of the *M*4.8 earthquake corresponding to Event D may not be necessarily equal to *M*4.3 but smaller. *Ye et al*. [2012] picked up “the possible repeating earthquakes” off Kamaishi based on magnitude (*M*4.3–*M*5.9) in addition to the hypocenter locations, which may miss the earthquakes that correspond to Event D. Therefore, it is important to focus on earthquakes smaller than repeaters by using high-frequency records [e.g., *Imanishi and Ellsworth*, 2013] to understand the partial rupturing of asperities.

For laws other than the aging law, the simulation results show that the Nagata law cannot reproduce the observed temporal aperiodicity, which indicates that the value of parameter c may be lower than the adopted value ($c = 2$) if the Nagata law holds because $c = 0$ for the Nagata law is equivalent to the aging law. If the slip law holds, seismic quiescence is expected to occur after the passage of large postseismic slip, which indicates that the temporal earthquake aperiodicity off Kamaishi may be caused by a chain reaction of many asperities [*Matsuzawa et al*., 2004]. Future studies should confirm these possibilities.

Before the 2011 Tohoku earthquake, there was quiescence of repeaters in and around the source region [*Uchida and Matsuzawa*, 2011]. Considering the slip behavior of NSA in Figure 2a, we infer that the region where nonsimilar earthquakes occur without repeaters may reflect a stress shadow due to strong plate coupling where great earthquakes will occur.

From observational results [e.g., *Uchida et al*., 2009], the slip amount estimated from repeating earthquake analyses tends to be smaller than that estimated from GPS analyses for large amounts of postseismic slip [*Ariyoshi et al*., 2007]. Our simulation results show the nonsimilar earthquakes, which are not counted as slip amount of the repeating earthquakes, occur in the passage of postseismic slip due to the whole rupturing and partial rupturing with fluctuated location of focal area. Therefore, the possible repeating earthquakes should be counted as the slip amount of repeating earthquake analyses.

These estimations are independent of rock laboratory experiments [e.g., *Blanpied et al*., 1998] and geodetic analyses [e.g., *Ozawa et al*., 2011], which would be useful to develop constitutive friction laws and estimate slip amount more robustly.

5. Conclusions

We conclude that (i) a mixture of partial and whole rupturing of a single asperity can explain some of the observed variability in timing and size of the repeating earthquakes off Kamaishi, which cause the possible repeating earthquakes as described by *Ye et al*. [2012], and (ii) the nonsimilar (possible repeating) earthquakes should be counted as the slip amount of repeating earthquake analyses in order to avoid underestimation by excluding them because of low cross-correlation coefficient due to the perturbation of the ruptured area.

Focusing on the temporal earthquake aperiodicity immediately after megathrust earthquakes is critical in estimating friction laws and properties, because (iii) the partial rupturing can be reproduced with moderate frictional instability controlled by the values of $(b - a)$ and d_c only for the aging law of the RSF and not the slip or Nagata laws at least in case of our simplified model, (iv) detailed analysis of the slip distribution for aftershocks larger than the characteristic earthquake may reveal the region of frictional instability covering the characteristic earthquake, (v) precise hypocenter determination of aftershocks with magnitude smaller than the characteristic earthquake may give a clue to detect amplified earthquake clusters and the direction of large postseismic slip propagation, and (vi) the precise identification of the repeater quiescence region where nonsimilar earthquakes typically occur may help to estimate the strong plate coupling of megathrust earthquakes in advance.

Acknowledgments
Discussion with D. Kalafat and A. Pinar through the SATREPS project "Earthquake and Tsunami Disaster Mitigation in the Marmara region and Disaster Education in Turkey" (MAR-Dim) was fruitful. Two anonymous reviewer's comment helped us to improve our manuscript significantly. We deeply thank the editor for expeditious handling our submission. The present study used the Earth Simulator and the supercomputing resources at the Cyberscience Center of Tohoku University. The GMT software [*Wessel and Smith*, 1998] was used to draw a number of the figures. T. Baba kindly provided bathymetric data off Tohoku. This study was also partly supported by MEXT for Young Scientists (B), 23710212, 2013, the DONET project, and the research project for compound disaster mitigation on the great earthquakes and tsunamis around the Nankai trough region.

The Editor thanks two anonymous reviewers for their assistance in evaluating this paper.

References

Ampuero, J.-P., and A. M. Rubin (2008), Earthquake nucleation on rate state faults—Aging and slip laws, *J. Geophys. Res.*, *113*, B01302, doi:10.1029/2007JB005082.

Ariyoshi, K., T. Matsuzawa, R. Hino, and A. Hasegawa (2007), Triggered non-similar slip events on repeating earthquake asperities: Results from 3D numerical simulations based on a friction law, *Geophys. Res. Lett.*, *34*, L02308, doi:10.1029/2006GL028323.

Blanpied, M. L., C. J. Marone, D. A. Lockner, J. D. Byerlee, and D. P. King (1998), Quantitative measure of the variation in fault rheology due to fluid-rock interactions, *J. Geophys. Res.*, *103*, 9691–9712, doi:10.1029/98JB00162.

Boatwright, J., and M. Cocco (1996), Frictional constraints on crustal faulting, *J. Geophys. Res.*, *101*, 13,895–13,909, doi:10.1029/96JB00405.

Chen, K. H., R. Bürgmann, R. M. Nadeau, T. Chen, and N. Lapusta (2010), Postseismic variations in seismic moment and recurrence interval of repeating earthquakes, *Earth Planet. Sci. Lett.*, *299*, 118–125, doi:10.1016/j.epsl.2010.08.027.

Diao, F., X. Xiong, R. Wang, Y. Zheng, T. R. Walter, H. Weng, and J. Li (2013), Overlapping post-seismic deformation processes: Afterslip and viscoelastic relaxation following the 2011 M_w 9.0 Tohoku (Japan) earthquake, *Geophys. J. Int.*, *196*(1), 218–229, doi:10.1093/gji/ggt376.

Dieterich, J. H. (1979), Modeling of rock friction. 1, Experimental results and constitutive equations, *J. Geophys. Res.*, *84*, 2161–2168, doi:10.1029/JB084iB05p02161.

Fukuda, J., A. Kato, N. Kato, and Y. Aoki (2013), Are the frictional properties of creeping faults persistent? Evidence from rapid afterslip following the 2011 Tohoku-Oki earthquake, *Geophys. Res. Lett.*, *40*, 3613–3617, doi:10.1002/grl.50713.

Hori, T., and S. Miyazaki (2010), Hierarchical asperity model for multiscale characteristic earthquakes: A numerical study for the off-Kamaishi earthquake sequence in the NE Japan subduction zone, *Geophys. Res. Lett.*, *37*, L10304, doi:10.1029/2010GL042669.

Igarashi, T., T. Matsuzawa, N. Umino, and A. Hasegawa (2001), Spatial distribution of focal mechanisms for interplate and intraplate earthquakes associated with the subducting Pacific plate beneath the northeastern Japan arc: A triple-plated deep seismic zone, *J. Geophys. Res.*, *106*, 2177–2191, doi:10.1029/2000JB900386.

Imanishi, K., and W. L. Ellsworth (2013), Source scaling relationships of microearthquakes at Parkfield, CA, Determined using the SAFOD Pilot Hole Seismic Array, in *Earthquakes: Radiated Energy and the Physics of Faulting*, edited by R. Abercrombie et al., AGU, Washington, D. C., doi:10.1029/170GM10.

Johnson, K. M. (2013), Is stress accumulating on the creeping section of the San Andreas Fault?, *Geophys. Res. Lett.*, *40*, 6101–6105, doi:10.1002/2013GL058184.

Kame, N., S. Fujita, M. Nakatani, and T. Kusakabe (2012), Effects of a revised rate- and state-dependent friction law on aftershock triggering model, *Tectonophysics*, *600*, 187–195, doi:10.1016/j.tecto.2012.11.028.

Kame, N., S. Fujita, M. Nakatani, and T. Kusakabe (2013), Earthquake cycle simulation with a revised rate- and state-dependent friction law, *Tectonophysics*, *600*, 196–204, doi:10.1016/j.tecto.2012.11.029.

Kato, A., K. Obara, T. Igarashi, H. Tsuruoka, S. Nakagawa, and N. Hirata (2012), Propagation of slow slip leading up to the 2011 M_w 9.0 Tohoku-Oki earthquake, *Science*, *335*(6069), 705–708, doi:10.1126/science.1215141.

Kato, N. (2007), Expansion of aftershock areas caused by propagating post-seismic sliding, *Geophys. J. Int.*, *168*, 797–808.

Matsuzawa, T., T. Igarashi, and A. Hasegawa (2002), Characteristic small-earthquake sequence off Sanriku, northeastern Honshu, Japan, *Geophys. Res. Lett.*, *29*(11), 1543, doi:10.1029/2001GL014632.

Matsuzawa, T., N. Uchida, T. Igarashi, T. Okada, and A. Hasegawa (2004), Repeating earthquakes and quasi-static slip on the plate boundary east off northern Honshu, Japan, *Earth Planets Space*, *56*(8), 803–811, doi:10.1186/BF03353087.

Mitsui, Y., N. Kato, Y. Fukahata, and K. Hirahara (2012), Megaquake cycle at the Tohoku subduction zone with thermal fluid pressurization near the surface, *Earth Planet. Sci. Lett.*, *325-326*, 21–26, doi:10.1016/j.epsl.2012.01.026.

Nagata, K., M. Nakatani, and S. Yoshida (2012), A revised rate- and state-dependent friction law obtained by constraining constitutive and evolution laws separately with laboratory data, *J. Geophys. Res.*, *117*, B02314, doi:10.1029/2011JB008818.

Ozawa, S., T. Nishimura, H. Suito, T. Kobayashi, M. Tobita, and T. Imakiire (2011), Coseismic and postseismic slip of the 2011 magnitude-9 Tohoku-Oki earthquake, *Nature*, *475*, 373–376, doi:10.1038/nature10227.

Ruina, A. L. (1983), Slip instability and state variable friction laws, *J. Geophys. Res.*, *88*, 10,359–10,370, doi:10.1029/JB088iB12p10359.

Sakoi, H., T. Matsuyama, T. Hirayama, I. Yamazaki, and T. Yamamoto (2012), Moderate repeating earthquakes off Kushiro, eastern Hokkaido, Japan [written in Japanese with abstract and figure caption in English], *J. Seismol. Soc. Jpn. Ser., 2*, *65*, 151–161, doi:10.4294/zisin.65.151.

Shimamura, K., T. Matsuzawa, T. Okada, N. Uchida, T. Kono, and A. Hasegawa (2011a), Similarities and differences in the rupture process of the M ~ 4.8 repeating-earthquake sequence off Kamaishi, northeast Japan: Comparison between the 2001 and 2008 events, *Bull. Seismol. Soc. Am.*, *101*, 2355–2368.

Shimamura, K., T. Matsuzawa, T. Okada, and N. Uchida (2011b), The rupture process of an earthquake on March 20, 2011 in the source area of the repeating earthquakes off Kamaishi, NE Japan, and its relation to the M9.0 Tohoku earthquake, Abstract S43C-2274 presented at 2011 Fall Meeting, AGU, San Francisco, Calif., 5–9 Dec.

Tamaribuchi, K., Y. Yamada, Y. Ishigaki, and Y. Takagi (2010), Characteristic earthquake sequences near Miyakojima Island, Ryukyu Arc, Japan [written in Japanese with abstract and figure caption in English], *J. Seismol. Soc. Jpn. Ser., 2*, *62*, 193–207.

The Headquarters for Earthquake Research Promotion (2004), Evaluations of occurrence potentials or subduction-zone earthquakes to date [written in Japanese]. [Available at http://www.jishin.go.jp/main/chousa/04feb_hyuganada/index.html.]

Thomas, M. Y., N. Lapusta, H. Noda, and J.-P. Avouac (2014), Quasi-dynamic versus fully dynamic simulations of earthquakes and aseismic slip with and without enhanced coseismic weakening, *J. Geophys. Res. Solid Earth*, *119*, 1986–2004, doi:10.1002/2013JB010615.

Uchida, N., and T. Matsuzawa (2011), Coupling coefficient, hierarchical structure, and earthquake cycle for the source area of the 2011 off the Pacific coast of Tohoku earthquake inferred from small repeating earthquake data, *Earth Planets Space*, *63*(7), 675–679, doi:10.5047/eps.2011.07.006.

Uchida, N., T. Matsuzawa, W. L. Ellsworth, K. Imanishi, T. Okada, and A. Hasegawa (2007), Source parameters of a M4.8 and its accompanying repeating earthquakes off Kamaishi, NE Japan—Implications for the hierarchical structure of asperities and earthquake cycle, *Geophys. Res. Lett.*, *34*, L20313, doi:10.1029/2007GL031263.

Uchida, N., S. Yui, S. Miura, T. Matsuzawa, A. Hasegawa, Y. Motoya, and M. Kasahara (2009), Quasi-static slip on the plate boundary associated with the 2003 M8.0 Tokachi-Oki and 2004 M7.1 off-Kushiro earthquakes, Japan, *Gondwana Res.*, *16*, 527–533.

Wessel, P., and W. H. F. Smith (1998), New improved version of the Generic Mapping Tools released, *Eos Trans. AGU*, *79*, 579, doi:10.1029/98EO00426.

Yagi, Y., and Y. Fukahata (2011), Rupture process of the 2011 Tohoku-Oki earthquake and absolute elastic strain release, *Geophys. Res. Lett.*, *38*, L19307, doi:10.1029/2011GL048701.

Yamanaka, Y., and M. Kikuchi (2003), Source process of the recurrent Tokachi-Oki earthquake on September 26, 2003, inferred from teleseismic body waves, *Earth Planets Space*, *55*(12), e21–e24, doi:10.1186/BF03352479.

Ye, L., T. Lay, and H. Kanamori (2012), The Sanriku-Oki low-seismicity region on the northern margin of the great 2011 Tohoku-Oki earthquake rupture, *J. Geophys. Res.*, *117*, B02305, doi:10.1029/2011JB008847.